Article

Elemental distribution of surface sediments around Oki Trough including adjacent terrestrial area: Strong impact of Japan Sea Proper Water on silty and clayey sediments

Atsuyuki Ohta[1*], Noboru Imai[1], Shigeru Terashima[1], Yoshiko Tachibana[1],
Ken Ikehara[1] and Hajime Katayama[1]

Abstract: Four-hundred sixty marine sediment samples were collected in the western Sea of Japan and analyzed for 53 elements for a marine geochemical mapping project associated with a nationwide terrestrial geochemical map. Grain size and chemical compositions of marine sediments vary significantly with location of origin (shelf, marginal terrace, slope, or basin). Sandy sediments distributed on the shelf do not likely reflect the geochemical features of river sediments, which are the dominant source of sands in the shelf. Most of the shelf sediments sampled are composed of relict sediments (little contribution of stream sediments) formed between the regression age and the transgression age because they contain a large amount of quartz coated by iron hydroxide and highly enriched in As. The marginal terrace is covered by modern silty sediments that are selectively deposited at the water mass boundary between Tsushima Current (surface water) and Japan Sea Proper Water (deep water). Silty sediments in the western portion of marginal terrace are highly enriched in Nb, rare earth elements, Ta, and Th, which are supplied from Quaternary alkaline volcanic rocks by a denudation process. They are carried eastward by as much as 200 km by oceanic currents. In contrast, the eastern marginal terrace is covered by silty sediments that are highly abundant in Cu, Zn, and Hg, which is attributed to biogenic remains in sediments (organic complex formation). Clayey sediments are widely distributed in the Oki Trough and basin where a hemi-pelagic environment and highly oxic conditions are found because of the influence of Japan Sea Proper Water. A thin Mn oxide layer in the uppermost 0−4 cm and extreme enrichment of V, Co, Ni, Mo, Sb, and Pb would be caused by an early diagenetic process. Thus, the spatial distribution patterns of elements in marine sediments in the study area are strongly controlled by their depositional environments.

Keywords: geochemical mapping, marine sediment, stream sediment, Oki Trough, relict sediment, early diagenetic process, Japan Sea Proper Water

1. Introduction

A geochemical map that shows the spatial distribution of elements on the Earth's surface provides fundamental geo-information about an element's cycle in the upper crust, environmental assessment, and mineralogical exploration (Webb *et al*., 1978; Howarth and Thornton, 1983; Weaver *et al*., 1983). Recently, global-scale geochemical mapping has been an area of active study (Darnley *et al*., 1995; Salminen *et al*., 2005; De Vos *et al*., 2006). In contrast, the Geological Survey of Japan, National Institute of Advanced Industrial Science and

Technology (AIST) has uniquely prepared geochemical maps of 53 elements both in terrestrial and coastal sea areas in Japan mainly for environmental assessment (Imai *et al*., 2010) because Japan is surrounded by vast seas. Furthermore, we have proposed that a comprehensive geochemical map can be used as powerful tool to provide us information about elemental transportation and diffusive process from terrestrial areas to coastal seas or in marine environments (Ohta *et al*., 2007; Ohta *et al*., 2010; Ohta and Imai, 2011).

Rivers flowing to the western Sea of Japan are small, so elemental transfer from land to sea is very restricted in area.

[1]AIST, Geological Survey of Japan, Research Institute of Geology and Geoinformation

[*]Corresponding author: Atsuyuki Ohta, Central 7, 1-1-1 Higashi, Tsukuba, Ibaraki 305-8567, Japan. Email: a.ohta@aist.go.jp

In general, modern sedimentation process on the Sea of Japan side are dominated by silt and clay deposition on the marginal terrace, slope, and basins, and the shallow seafloor is covered in sandy sediments that are relict sediments from the last glacial stage and the subsequent transgression (Ikehara, 1991). Yin *et al.* (1987) pointed out that illite in the southern Sea of Japan is transported by the Tsushima Current from the East China Sea. However, Ohta *et al.* (2013) suggested that muddy sediments on the shelf of the eastern Tsushima Strait have homogenous chemical compositions and little contribution of Korean and Chinese terrigenous materials. Thus, it is still unclear what process controls the spatial distribution of elements in marine sediments in the Sea of Japan.

In this study, we selected the area around Oki Trough bordered on the east by the eastern Tsushima Strait. The submarine geology in the area has been examined using seismic reflection profiles as described the follow by Ikehara *et al.* (1990b), Yamamoto (1991), and Yamamoto (1993). The sediments were deposited in the marginal terrace during the late Pliocene to Holocene, and their thickness increases northwestward. In contrast, the shelf was an erosional surface during the Pliocene age. The southwestern region of the Oki Trough is covered by mass-transport deposits derived from the surrounding marginal terrace, but hemi-pelagic deposition is dominant in the northeastern part of the trough. The study area is thus characterized by a shelf having little contribution of adjacent terrestrial materials, a wide marginal terrace with thick sedimentary layers, and a hemi-pelagic basin associated partly with turbidites. The purpose of this study is to examine the controlling factors of spatial distribution patterns of marine sediments across various depositional environments using a comprehensive geochemical map.

2. Samples and methods

2.1　Marine environment study areas, sampling methods, and processing

Figures 1a and b present geographical names of the area and our sampling locations, respectively. The sea shelf, which is shallower than 200 m, is wide on the western end. Oki Strait is located on the west side of the study area. Small basins found on the southeast and southwest sides of Oki Islands are covered by silty sediment. Oki Spur is the topographic rise that continues from the Oki Strait. The Tsushima Warm Current flows from west to east with a complicated flow pattern (Naganuma, 1977). A branch of the current flows through the Oki Strait and along the coast, and the other branch flows on the northern side of Oki Spur. The Oki Ridge is the topographic rise 300−500 m below the surface of the sea and forms the boundary between the Yamato Basin and the Oki Trough. The marginal terrace is

a wide terrace with a water depth of 200−500 m (Iwabuchi 1968; Iwabuchi and Kato, 1988). The Oki Trough is a deep sea basin with a depth of 900−1750 m below the surface of the sea and which declines gently toward northeast. Wakasa Bay has a deeply indented coastline, along which the coastal current flows from west to east. Wakasa Basin is a small basin located next to Oki Trough. Wakasa Sea Knoll Chain and Gentatsu-Se are small seafloor topographic rises.

The 460 marine sediment samples used in this study were collected using a grab sampler during Cruises GH86-2 GH87-2 and GH88-2 in 1986, 1987, and 1988 respectively (Ikehara *et al*., 1990a; Katayama *et al*., 1993, 2000; Katayama and Ikehara, 2001; Ikehara, 2010). The sampling locations and particle sizes are presented in Fig. 1b. The median diameters of sediments, shown in Φ-scale (negative natural logarithm of grain diameter), were used for classifying the sediments. The sediments were classified into six groups according to texture: granule ($-2 < \Phi \leq -1$), very coarse-coarse sand ($-1 < \Phi \leq 1$), medium sand ($1 < \Phi \leq 2$), fine-very fine sand ($2 < \Phi \leq 4$), silt ($4 < \Phi \leq 8$), and clay ($8 < \Phi$). The uppermost 0−3 cm of the archived sediments collected with the grab sampler were separated, dried in air, ground with an agate mortar and pestle, and retained for analyses.

### 2.2　Terrestrial study areas, sampling methods, and processing

The terrestrial area has gentle relief and a limited flood plain to the west of Wakasa Bay but precipitous mountains in the northeast part of the study area. The rivers located in the western part of the study area have small mean flow rates of 1.0−1.5 km³/year. Hii, Kuzuryu, Sendai, Tetori, and Yura Rivers are major rivers in the terrestrial area (Fig. 1a). Kuzuryu and Tetori Rivers have the largest mean flow rates of 2.3−2.7 km³/year and carry the largest amount of sediments to the sea (4.7−6.8 ×10⁵ m³/year) in the study area (Akimoto *et al*., 2009). The Yura River also supplies a large amount of silty sediments of 4.4×10⁵ m³/year to Wakasa Bay.

Geochemical analyses from 246 stream sediment samples were used for comparison to the marine surface sediment geochemical data. These samples were collected from adjacent terrestrial areas during the period 1999−2002 for Japanese regional geochemical mapping, with a mean sampling density of one sample per 100 km². Eight samples were additionally collected from the Oki Islands in 2013. The stream sediments were dried in air and sieved using an 83 mesh (180 μm) screen. Unlike the marine samples, the stream sediment samples were not milled.

Figure 1b also presents a geologic map of the study area, simplified from the Geological Map of Japan 1:1,000,000 (Geological Survey of Japan, 1992). Granitic rocks intruded
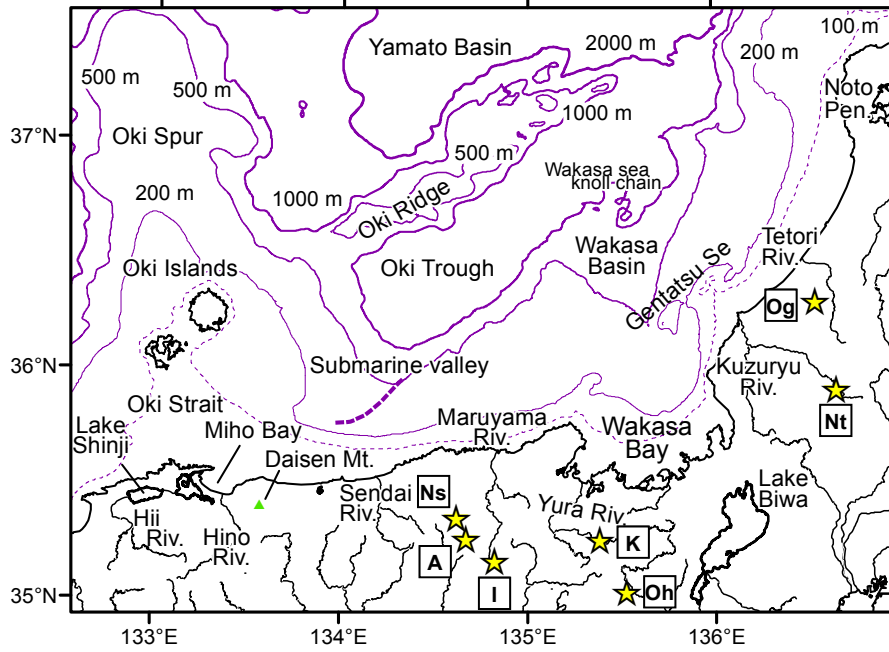
(Fig. 1a)
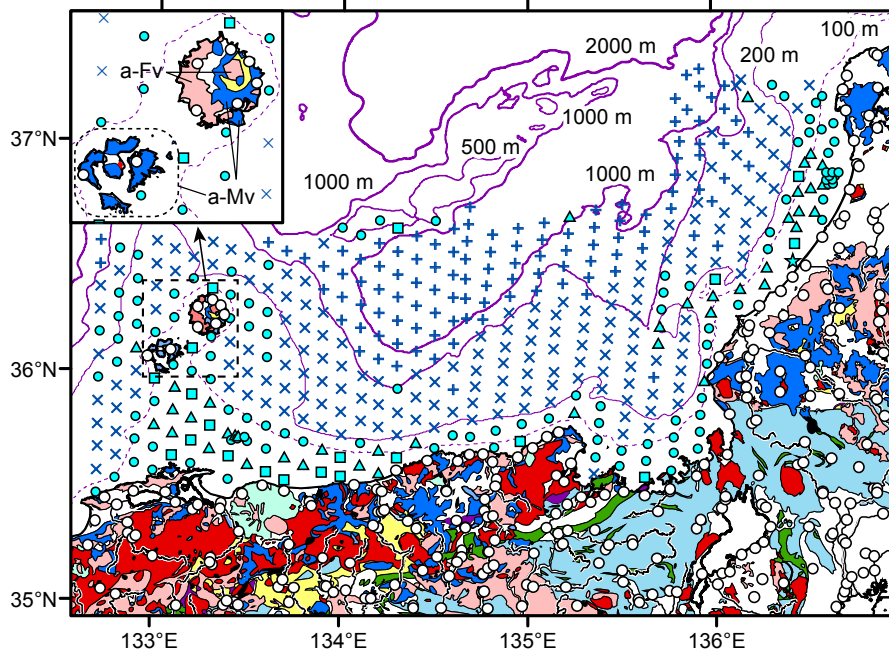
(Fig. 1b)
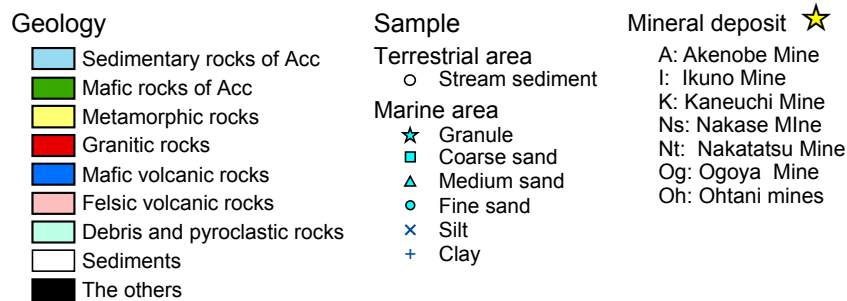
Fig. 1 Schematic maps of the study area. a) Geographical name map; solid lines in terrestrial areas show major rivers. b) Sampling locations of stream sediments and coastal sea sediments with surface geology. The abbreviations Acc, a-Fv, and a-Mv mean accretionary complexes, alkaline felsic volcanic rock, and alkaline mafic volcanic rock, respectively. Depth contours were delineated using a dataset provided by the Japan Oceanographic Data Center.

during the Cretaceous-Paleogene are distributed in the western part and around Lake Biwa. High-pressure-type metamorphic rocks around Sendai river and in the southern direction of Daisen Mountain dominantly consist of pelitic-, psammitic-, siliceous-, and basic schist. Alkaline volcanic rocks of Miocene age are dominantly distributed in the Oki Islands. Non-alkaline volcanic rocks consisting mainly of Miocene andesitic-dacitic rocks are distributed widely on the Sea of Japan side. They have a greenish color caused by conspicuous alteration and are known as Green-tuff. Daisen volcano consists of andesitic-dacitic lava and tuff formed by Quaternary volcanic activity. The central part of the study area has an old tectonic belt consisting of accretionary complexes of mélange, mudstone, sandstone, and exotic blocks (chert, limestone, greenstones, gabbro and ultramafic rocks), that range in age mainly through the Jurassic-Cretaceous. Permian-Triassic sedimentary rocks associated with limestone and mafic-ultramafic rock (Yakuno ophiolite) are distributed near Wakasa Bay. Sedimentary rocks distributed along the coast were deposited mainly during the Tertiary-Quaternary.

Figure 1a shows seven major mines in the study area. Ogoya (Cu-Zn-type), Nakatatsu (Zn- and Pb-type), and Kaneuchi (Sn- and W-type) mines are located in the catchment area of rivers flowing to the Sea of Japan. The Ohtani mine yields W and Sn ores. Nakase mine yields Au, Ag, and Sb. Akenobe and Ikuno mines are polymetallic-vein-type deposits.

2.3 Geochemical analysis

The analytical method including quality control has been described in Ohta *et al*. (2013). First, 0.2 g of each sample was digested for 2 h using HF, HNO_3, and $HClO_4$ solutions at 120 °C. The degraded product was evaporated to dryness at 200 °C; then the residue was dissolved with 100 mL of 0.35 M HNO_3 solution. Concentrations of 51 elements were determined using inductively coupled plasma atomic emission spectrometry (ICP-AES) for Na_2O, MgO, Al_2O_3, P_2O_5, K_2O, CaO, TiO_2, MnO, Total (T-) Fe_2O_3, V, Sr, and Ba, and using inductively coupled plasma mass spectrometry (ICP-MS) for Li, Be, Sc, Cr, Co, Ni, Cu, Zn, Ga, Rb, Zr, Nb, Y, Mo, Cd, Sn, Sb, Cs, La, Ce, Pr, Nd, Sm, Eu, Gd, Tb, Dy, Ho, Er, Tm, Yb, Lu, Hf, Ta, Tl, Pb, Bi, Th, and U. Analyses of As in all samples and Hg in stream sediment samples were subcontracted to ALS Chemex in Vancouver, B.C. Hg in marine sediments were determined using an MA-2000 (Nippon Instruments Corp.) that measures the quantity of Hg vapor generated by thermal decomposition using an atomic absorption spectrometer. A part of the heavy mineral fraction was not digested satisfactorily by HF, HNO_3, and $HClO_4$ solutions. Incomplete decomposition of these minerals affected the determination of some elemental abundance, especially of Zr and Hf included in zircon. In addition,

our marine sediments were not desalinated. Therefore, Zr and Ha in stream and marine sediments and Na in marine sediments should be used only as a guide. Tables 1 and 2 present summaries of the analytical results obtained for marine and stream sediments, respectively.

2.4 Spatial analyses

The spatial distribution patterns of elements in both the terrestrial and the marine environments of the study area were prepared using geographic information system (GIS) software (ArcGIS 10.2; Environmental Systems Research Institute, Inc. (ESRI)). The method is described in detail in Ohta *et al*. (2004). The inverse distance weight (IDW) method was used for interpolation of point data (Watson and Philip, 1985). Marine sediments and stream sediments differ in their chemical and mineralogical compositions, particle size, and origin. Therefore, a common class selection makes the regional geochemical differences (color variation) in either the terrestrial area or the marine area difficult to see (Ohta *et al*., 2007). Consequently, a class selection of elemental concentration is separated for terrestrial and marine environments. In this study, a percentile is used for class selection of elemental concentration intervals in maps: $0 \leq x \leq 5$, $5 < x \leq 10$, $10 < x \leq 25$, $25 < x \leq 50$, $50 < x \leq 75$, $75 < x \leq 90$, $90 < x \leq 95$, and $95 < x \leq 100\%$, where x represents the elemental concentration (Reimann, 2005). Using this class selection, geochemical patterns displayed in different sample media can be directly compared, independent of the actual element concentration (Reimann, 2005; Ohta *et al*., 2007).

The spatial distribution patterns of mud concentration and oxidative-reductive potential (ORP) in marine environment are also created. These data are taken from by Ikehara *et al*. (1990a), Katayama *et al*. (1993, 2000), Katayama and Ikehara (2001), and Ikehara (2010). The study area is widely covered by silt and clay and the median value of mud content is 77%. Thus, mud content classification was arbitrarily selected to be 20%, 40%, 60%, 80%, and 100%. ORP was measured for a surface sediment sample collected using a K-grab sampler on board ship and was not observed in-situ at the bottom of sea. The data were collected only in the summer season (mainly June to July). So the classification of ORP was also arbitrarily selected to be −100 eV, −50 eV 0 eV, 50 eV, 100 eV, 200 eV because ORP data are rather qualitative nature. The resulting spatial distribution of mud content, ORP, and typical examples of elemental concentrations are shown in Fig. 2.

Table 1 Summary for the geochemistry of marine sediments off eastern Tsushima Island, Japan ($N = 460$).

Element	unit	Min	25%	Median	Mean	75%	Max	MAD	S.D.
Na_2O	wt. %	1.08	2.38	2.83	3.33	3.86	9.70	0.58	1.49
MgO	wt. %	0.43	2.11	2.55	2.46	2.93	4.75	0.42	0.64
Al_2O_3	wt. %	2.00	8.18	9.29	9.13	10.2	13.9	0.97	1.61
P_2O_5	wt. %	0.032	0.107	0.131	0.137	0.155	0.713	0.024	0.063
K_2O	wt. %	0.51	1.79	1.95	1.94	2.10	3.55	0.16	0.30
CaO	wt. %	0.41	2.27	4.18	4.88	6.21	33.4	1.98	4.31
TiO_2	wt. %	0.077	0.317	0.386	0.378	0.437	1.93	0.056	0.126
MnO	wt. %	0.016	0.043	0.053	0.137	0.084	2.31	0.014	0.281
$T\text{-}Fe_2O_3$	wt. %	0.84	3.20	3.69	3.74	4.13	18.0	0.46	1.33
Li	mg/kg	5.64	32.9	44.8	46.4	56.4	96.3	11.7	18.4
Be	mg/kg	0.46	1.18	1.37	1.36	1.53	4.45	0.18	0.33
Sc	mg/kg	1.24	7.14	8.34	8.08	9.46	20.1	1.14	2.13
V	mg/kg	6.16	43.0	58.1	57.3	72.0	190	14.6	21.4
Cr	mg/kg	9.27	35.1	47.7	45.2	55.4	250	9.54	17.4
Co	mg/kg	1.36	6.80	8.41	8.65	9.80	27.8	1.47	3.22
Ni	mg/kg	3.11	13.8	23.4	23.7	32.8	129	9.50	12.4
Cu	mg/kg	2.47	9.20	21.9	28.5	40.6	144	14.0	24.2
Zn	mg/kg	14.70	62.2	83.3	80.0	99.0	154	17.7	25.6
Ga	mg/kg	3.58	12.2	13.6	13.3	14.8	22.8	1.23	2.15
As	mg/kg	0.2	4.2	6.6	8.0	10	58	2.7	7.0
Rb	mg/kg	17.3	62.0	70.9	69.7	77.9	156	8.21	14.6
Sr	mg/kg	72	162	236	282	311	2152	75	240
Y	mg/kg	3.16	9.20	10.9	10.8	12.4	24.4	1.62	2.83
Zr	mg/kg	11	41	50	50	57	127	7	17
Nb	mg/kg	1.77	5.72	7.13	7.45	8.36	20.4	1.35	2.88
Mo	mg/kg	0.23	0.60	0.82	1.67	1.20	32.6	0.25	3.21
Cd	mg/kg	0.019	0.046	0.061	0.070	0.082	0.30	0.017	0.038
Sn	mg/kg	0.36	1.45	2.00	1.90	2.35	4.02	0.41	0.61
Sb	mg/kg	0.20	0.49	0.63	0.76	0.94	3.28	0.20	0.44
Cs	mg/kg	0.26	2.72	3.91	3.88	5.21	9.75	1.28	1.56
Ba	mg/kg	60.0	296	337	347	377	2226	40.9	125
La	mg/kg	4.92	14.1	16.3	16.8	18.9	63.1	2.36	5.29
Ce	mg/kg	12.1	28.1	33.3	34.3	39.2	146	5.68	12.0
Pr	mg/kg	1.01	3.28	3.78	3.83	4.34	14.0	0.52	1.20
Nd	mg/kg	3.94	12.6	14.6	14.8	16.8	54.5	2.06	4.59
Sm	mg/kg	0.78	2.46	2.86	2.85	3.25	10.3	0.40	0.84
Eu	mg/kg	0.26	0.56	0.65	0.66	0.72	2.22	0.081	0.16
Gd	mg/kg	0.67	2.17	2.53	2.50	2.85	8.36	0.34	0.70
Tb	mg/kg	0.11	0.35	0.41	0.40	0.46	1.20	0.053	0.11
Dy	mg/kg	0.55	1.73	2.00	1.96	2.24	5.13	0.26	0.49
Ho	mg/kg	0.098	0.32	0.38	0.37	0.42	0.88	0.048	0.090
Er	mg/kg	0.30	0.94	1.09	1.06	1.21	2.43	0.13	0.25
Tm	mg/kg	0.049	0.15	0.17	0.17	0.19	0.36	0.022	0.04
Yb	mg/kg	0.31	0.92	1.06	1.04	1.19	2.09	0.13	0.23
Lu	mg/kg	0.045	0.14	0.16	0.15	0.17	0.29	0.018	0.03
Hf	mg/kg	0.31	1.1	1.3	1.3	1.5	3.1	0.18	0.39
Ta	mg/kg	0.036	0.51	0.65	0.65	0.77	1.46	0.13	0.22
Hg	µg/kg	0.5	35	62	70	100	400	32	48
Tl	mg/kg	0.036	0.44	0.49	0.48	0.53	0.83	0.046	0.091
Pb	mg/kg	9.86	20.9	25.1	27.3	31.7	86.4	4.88	9.93
Bi	mg/kg	0.071	0.23	0.40	0.42	0.59	1.08	0.18	0.23
Th	mg/kg	1.58	4.97	6.12	6.07	7.10	29.9	1.04	1.94
U	mg/kg	0.43	1.12	1.38	1.40	1.65	3.66	0.26	0.41

Minimum (Min), maximum (Max), median absolute deviation (MAD) and standard deviation (S.D.)
As: 11 samples below D.L. (0.2 mg/kg); Hg: 6 samples below D.L. (0.5 µg/kg)

Table 2　Summary for the geochemistry of stream sediments ($N = 254$).

Element	unit	Min.	25%	Median	Mean	75%	Max.	MAD	S.D.
Na$_2$O	wt. %	0.71	1.59	2.02	2.07	2.56	4.07	0.44	0.68
MgO	wt. %	0.37	1.56	2.08	2.39	2.94	10.87	0.65	1.27
Al$_2$O$_3$	wt. %	4.39	8.28	10.27	10.44	12.15	19.17	1.94	2.67
P$_2$O$_5$	wt. %	0.033	0.096	0.12	0.13	0.15	0.47	0.028	0.062
K$_2$O	wt. %	0.80	1.81	2.15	2.10	2.38	3.76	0.28	0.47
CaO	wt. %	0.14	0.93	1.56	1.80	2.48	5.17	0.78	1.12
TiO$_2$	wt. %	0.16	0.56	0.68	0.80	0.84	3.13	0.13	0.45
MnO	wt. %	0.029	0.093	0.12	0.13	0.15	1.10	0.031	0.082
T-Fe$_2$O$_3$	wt. %	1.34	4.32	5.29	5.73	6.65	18.1	1.18	2.17
Li	mg/kg	9.9	25.2	33.0	34.7	41.3	89.1	8.1	12.5
Be	mg/kg	0.53	1.41	1.69	1.76	2.02	4.05	0.29	0.53
Sc	mg/kg	2.77	7.80	10.3	11.5	14.4	36.0	3.06	5.02
V	mg/kg	20.2	78.3	100	114	136	378	29.2	54.4
Cr	mg/kg	14.1	41.5	60.7	94.4	97.2	1941	23.5	140
Co	mg/kg	2.53	10.5	13.4	15.1	18.0	59.7	3.66	7.64
Ni	mg/kg	4.99	16.1	25.4	38.2	38.9	699	10.8	59.6
Cu	mg/kg	5.66	21.0	29.9	52.1	44.1	2599	10.5	167
Zn	mg/kg	17.1	99.7	126	214	157	11444	28.2	743
Ga	mg/kg	11.7	16.0	17.2	17.4	18.7	26.2	1.36	2.30
As	mg/kg	1.0	6.0	10	25	19	1578	5.0	107
Rb	mg/kg	17.6	68.8	93.4	93.6	116	186	23.1	35.4
Sr	mg/kg	25.1	86.5	131	144	180	597	47.1	84.1
Y	mg/kg	5.40	12.8	15.9	17.3	21.3	47.0	4.01	6.90
Zr	mg/kg	19.1	45.4	57.1	64.0	67.6	367	11.0	41.5
Nb	mg/kg	4.10	6.94	8.14	9.93	9.94	77.2	1.45	8.28
Mo	mg/kg	0.35	0.82	1.11	1.39	1.58	9.71	0.36	1.09
Cd	mg/kg	0.045	0.13	0.19	0.42	0.29	28.7	0.073	1.88
Sn	mg/kg	0.94	2.31	3.01	5.27	3.98	170	0.80	12.9
Sb	mg/kg	0.17	0.54	0.85	1.44	1.22	63.7	0.32	4.28
Cs	mg/kg	1.41	3.23	4.57	5.10	6.03	16.0	1.44	2.71
Ba	mg/kg	210	369	439	447	506	1649	69	129
La	mg/kg	11.1	17.5	20.4	23.7	24.8	119	3.7	12.6
Ce	mg/kg	19.6	32.3	37.1	44.0	46.6	232	6.5	24.6
Pr	mg/kg	2.59	4.00	4.67	5.35	5.66	25.9	0.79	2.70
Nd	mg/kg	10.1	15.6	18.2	20.7	22.3	92.7	2.91	9.68
Sm	mg/kg	1.79	3.12	3.56	3.99	4.34	16.1	0.58	1.71
Eu	mg/kg	0.37	0.66	0.79	0.80	0.92	2.48	0.13	0.22
Gd	mg/kg	1.44	2.72	3.19	3.48	3.89	11.4	0.57	1.33
Tb	mg/kg	0.23	0.44	0.54	0.57	0.65	1.36	0.10	0.20
Dy	mg/kg	1.07	2.22	2.72	2.90	3.35	7.10	0.58	1.10
Ho	mg/kg	0.19	0.41	0.52	0.55	0.65	1.38	0.12	0.21
Er	mg/kg	0.56	1.21	1.49	1.62	1.97	4.28	0.35	0.62
Tm	mg/kg	0.09	0.19	0.24	0.26	0.31	0.70	0.05	0.10
Yb	mg/kg	0.55	1.21	1.50	1.62	1.92	4.58	0.34	0.64
Lu	mg/kg	0.08	0.17	0.22	0.24	0.28	0.69	0.05	0.09
Hf	mg/kg	0.59	1.35	1.63	1.76	1.86	8.16	0.26	0.88
Ta	mg/kg	0.28	0.51	0.63	0.78	0.83	5.23	0.15	0.58
Hg	µg/kg	10	30	42	91	80	2660	25	240
Tl	mg/kg	0.12	0.49	0.61	0.64	0.73	2.52	0.12	0.27
Pb	mg/kg	10.1	21.2	25.9	63.9	34.2	4177	5.9	291
Bi	mg/kg	0.050	0.19	0.28	0.41	0.39	6.00	0.10	0.59
Th	mg/kg	2.11	5.40	7.12	9.25	9.74	53.6	2.09	7.34
U	mg/kg	0.63	1.33	1.69	1.89	2.12	8.90	0.40	1.00

Minimum (Min), maximum (Max), median absolute deviation (MAD) and standard deviation (S.D.)
As: 6 samples below D.L.(1.0 mg/kg); Hg: 13 samples below D.L.(10 µg/kg).

3. Results

3.1 Characteristics of marine surface sediments

Characteristics of grain size, mud content, and ORP in marine sediments are shown in Figs. 1b and 2a, respectively. Grain size and mud content in marine sediments decreases gradually in a seaward direction. ORP is positive on the shelf and around Oki Trough and negative on the marginal terrace and slope. Negative values at the mouths of the Maruyama, Yura, and Kuzuryu rivers indicate input of organic matter on land (Katayama *et al.*, 1993; 2000; Kondo, 2006). The continental shelf is covered predominantly by sandy sediments. Quartz particles covered by iron hydroxides are found in the eastern part of Oki Strait and the shelf off Noto Peninsula (Ikehara *et al.*, 1990a; Katayama and Ikehara, 2001). Quartz in modern sediments supplied from a river is not covered by iron hydroxides. Therefore, they are relict sediments deposited from regression age to transgression age. Sandy sediments (partly including sandy silt) having positive ORP and low mud content (< 60%) are also found in submarine valleys off Sendai River, around Gentatsu-Se, and at the Oki Ridge. The sandy sediments in the submarine valley and around Gentatsu-Se contain not newer volcanic glass and pumice (< 10 ky) but older ones (> 10 ky) (Ikehara *et al.*, 1990a; Katayama *et al.*, 2000). The sediments would be denudated from old sediments. Positive ORP data indicates that these places have quite low deposition rates or are in erosional regimes.

Silty sediments are widely distributed on the marginal terrace (WD = 200 – 400 m) and slope (WD = 400 – 900 m), and have more than 80% mud content. The small basins located at both sides of the Oki Strait (WD = 120 – 200 m) are covered by silty sediments having > 60% mud content. The Oki Trough is characterized by oxidative condition because the Japan Sea Proper Water (JSPW) flows from the Yamato Basin (Senjyu *et al.*, 2005). JSPW is the most homogenous water mass in the Sea of Japan at depths deeper than 300 m, and is characterized by low temperature (0 – 1 °C) and high oxygen concentrations (210 – 260 μmol/kg) (Gamo *et al.*, 1986; Sudo, 1986). JSPW accelerates the dissolution of calcareous material. The abundance of calcareous nano-plangtonic materials steeply decreases below water depths of 900 m and these materials are nearly absent below a water depth of 1250 m (Ikehara *et al.*, 1990a).

3.2 Marine spatial distribution patterns of elemental concentrations

Sandy and silty sediments around the Oki Spur and Oki Islands are enriched in CaO, P_2O_5, TiO_2, Cr, Sr, Nb, Cd, Ta, Y, lanthanides (Ln), and Th. Stream sediments in the Oki inlands are also enriched in P_2O_5, TiO_2, Nb, Mo, Cd, Y, Ln, Ta, Th and

U but poor in Li, MgO, CaO, Cs, Tl. High CaO and Sr concentrations on topographic heights are attributed to shell fragments and foraminifera. The small basins (WD = 120 – 200 m) located southeast and southwest of the Oki Islands are covered by silty sediments and enriched in Li, Be, Sc, Cr, Co, Ni, Cu, Ni, Zn, Ga, Nb, Cs, Sn, Cd, Pb, Hg, Bi, Tl, and U. Sandy sediments on the Oki Strait are composed dominantly of calcareous materials, quartz, plagioclase, and lithic fragments (Fig. 1b) (Ikehara, 2010). Most elements are poor in the Oki Strait and the shelf expanding westward from Oki Strait (depth of under 100 m). However Al_2O_3 is abundant around Miho Bay; CaO and Sr are enriched in the water off Sinji Lake and Daisen volcano; K_2O and Rb concentrations are low on the coastal zone (WD = 0 – 50 m) but are elevated offshore (WD = 50 – 200 m); As is highly rich in the eastern part of Oki Strait.

The Oki Trough and Wakasa Basin are highly enriched in MgO, P_2O_5, V, MnO, Co, Ni, Cu, As, Mo, Sn, Sb, Cs, Ba, Tl, Pb, and Bi. In contrast, Cu, Zn, and Hg are instead enriched in the slope around the Oki Trough and Wakasa Basin (WD = 200 – 900 m). CaO and Sr concentrations are quite low in these places because the lysocline is shallow (900 – 1250 m) in the Sea of Japan (Ikehara *et al.*, 1990a). The marginal terrace southwest and south of the Oki Trough is covered by silt and enriched in P_2O_5, Y, Nb, Ln, Ta, Th and U. Sandy sediments around the Oki Ridge and Wakasa Sea Knoll chain are enriched in Be, K_2O, $T-Fe_2O_3$, Sc, Cr, Ga, Rb, Y, Nb, Ba, Ln, Ta, and Th.

The sediments in the western part of Wakasa Bay have high mud contents and enriched in Al_2O_3, MgO, TiO_2, MnO, $T-Fe_2O_3$, Sc, V, Cr, Co, and Ni. The northern area of Wakasa Bay is a gradual slope (WD = 200 – 500 m) that is covered in silty sediments. In this region, many elements excluding for MgO, K_2O, CaO, Rb, Sr, Ba, and Tl are abundant. The Kaneuchi mine locating in the catchment area of Yura River is a Sn-W mine. It elevates MnO, Cu, Zn, As, Cd, Sn, Sb, and Pb concentrations in stream sediments. However, the influence of this mine to Wakasa Bay seems to be slight. The features of spatial distribution of elements in the Wakasa Basin are similar to those of the Oki Trough: MgO, P_2O_5, MnO, Li, V, Cr, Co, Ni, Cu, Zn, Mo, Cd, Sb, Bi, and Hg are abundant there.

The K_2O, TiO_2, MnO, $T-Fe_2O_3$, Ba, and As concentrations are sporadically high on the shelf off Noto Peninsula. The topographic high around Gentatsu-Se is abundant in CaO and Sr attributed to shell fragments. Fine and medium sands distributed around Gentatsu-Se were supplied by the Kuzuryu River and are abundant in Al_2O_3, K_2O, TiO_2, MnO, $T-Fe_2O_3$, Be, Sc, V, Co, Ba, and Ln. The Ogoya and Nakatatsu Mines are Cu-Zn-type and Zn-Pb-type mines, respectively. They elevate Cu, Zn, Cd, Mo, Sb, Pb, and Bi concentrations in stream sediments collected near these mines. However, the adjacent coastal sea
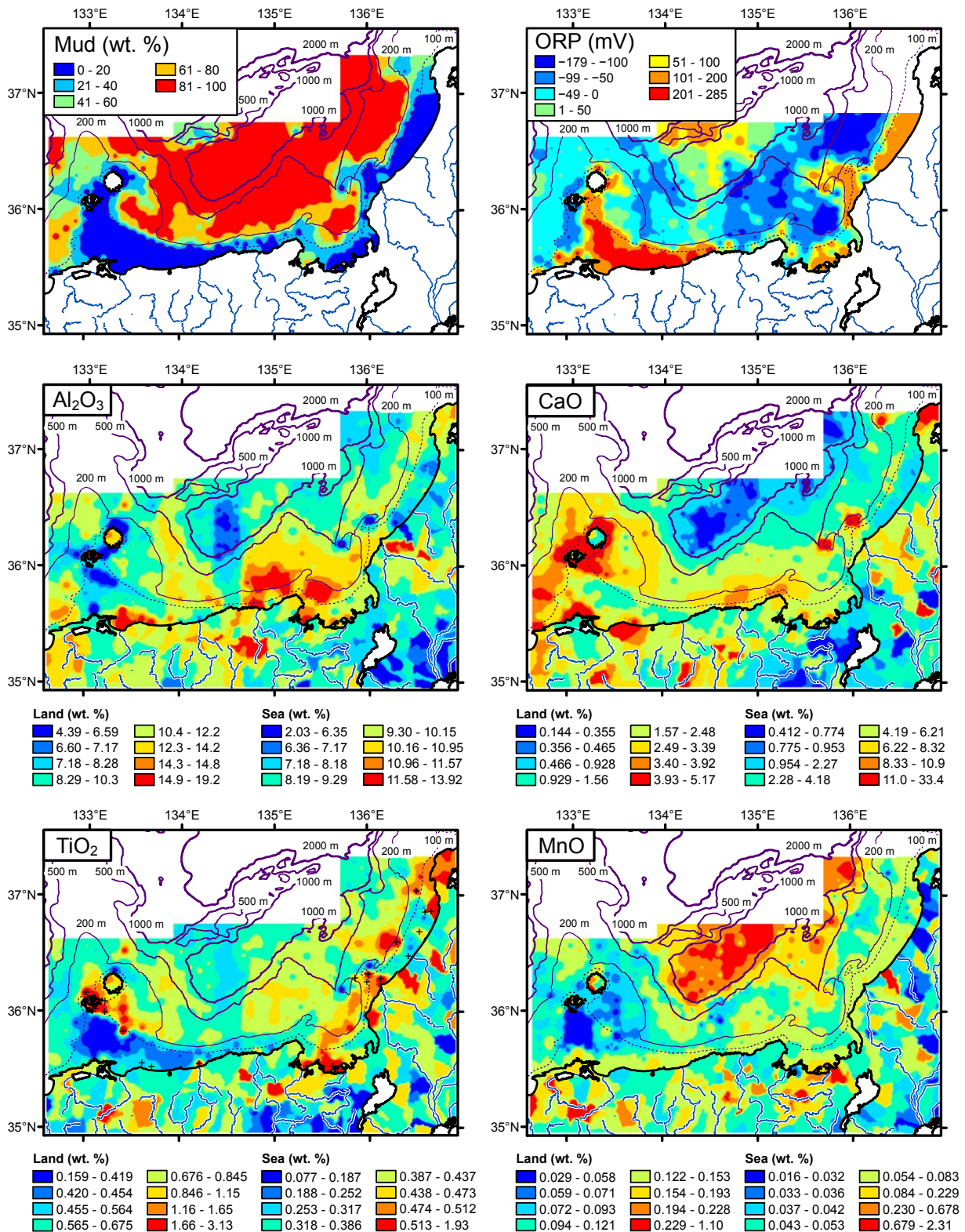
(Fig. 2a)

Fig. 2 Spatial distributions of mud (silt + clay) content and ORP data in marine areas and those of elemental concentrations in terrestrial and marine areas for Al₂O₃, CaO, TiO₂, MnO, T-Fe₂O₃, Cr, Cu, As, Nb, Cd, Cs, La, Hg and Pb data. Star symbols indicate major metalliferous deposits. Cross symbols indicate samples containing brown or brownish black sands. Plus symbols indicate samples that plot outside the positive correlation between elemental concentrations and median diameter (Fig. 3).

(Fig. 2b)
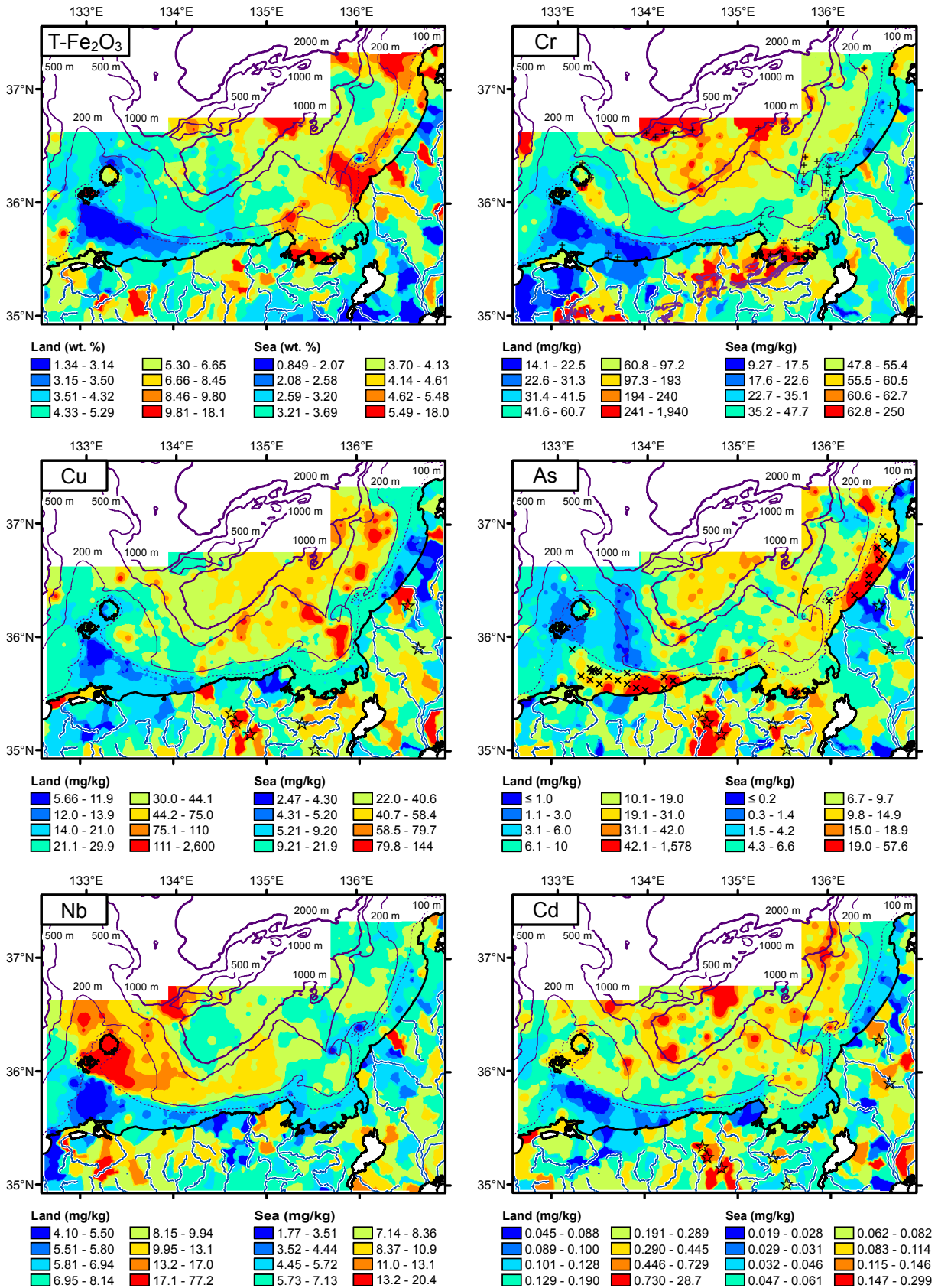
Fig. 2 Continued.

(Fig. 2c)
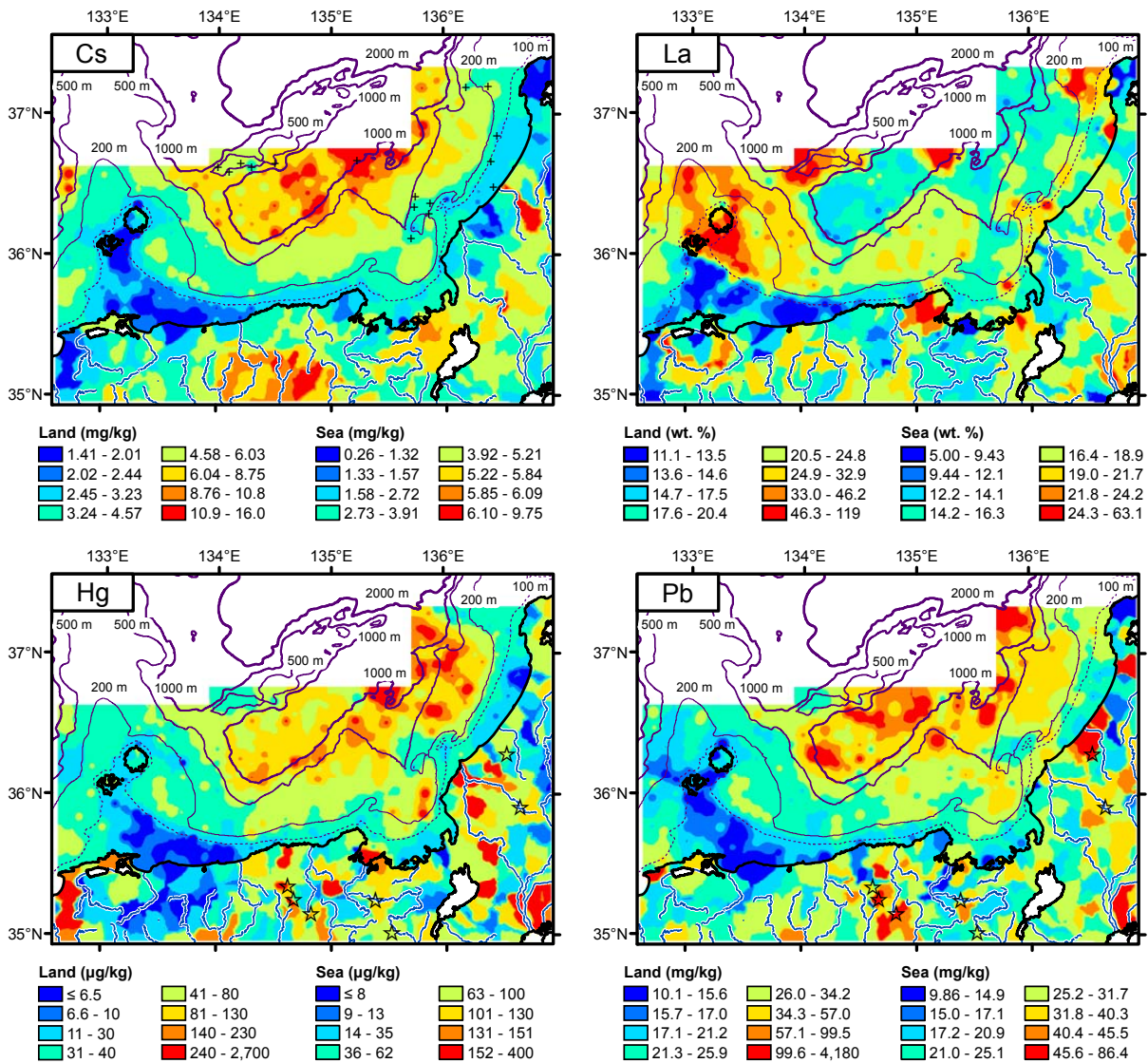
Fig. 2 Continued.

sediments are not abundant in these elements.

3.3 Variation of elemental concentrations in marine sediments with grain size or with water depth

Elemental concentrations in marine sediments change significantly with grain size (Ohta and Imai, 2011). It is necessary to examine the influence of grain size on elemental concentrations to elucidate the element transfer process in the marine environment. This is because coarse sediments on the shelf or topographic highs are enriched in quartz and calcareous materials, which dilutes the concentrations of most elements except for SiO_2, CaO, and Sr. Figure 3 shows the relationships between the concentrations of 12 elements and median diam-

eter (Φ). In addition, median elemental concentrations of 53 elements of marine sediments are summarized in Table 3.

The concentrations of all elements except for As increase sharply from $\Phi = -2$ to $\Phi = 4$ because of the dilution effect by quartz and calcareous materials. Be, K_2O, Al_2O_3, TiO_2, $T\text{-}Fe_2O_3$, Sc, Ga, Rb, Sr, Nb, Sn, Y, Ba, Ln, Ta, Th, and U concentrations are constant from $\Phi = 4$ to $\Phi = 7-8$, followed by a gradual (but slight) decrease in the $\Phi > 7-8$ range (see Al_2O_3, TiO_2, and Nb in Fig. 3). CaO and Sr follow trends similar to Al_2O_3 except for sediments on the shelf, which contain more than 10 wt. % CaO. MgO, P_2O_5, V, Cr, Co, Cu, Zn, Mo, Cd, Sn, Sb, Cs, Hg, Pb, and Bi concentrations increase with decreasing grain size (see Cs in Fig. 3). The relationship between As concentration and grain size
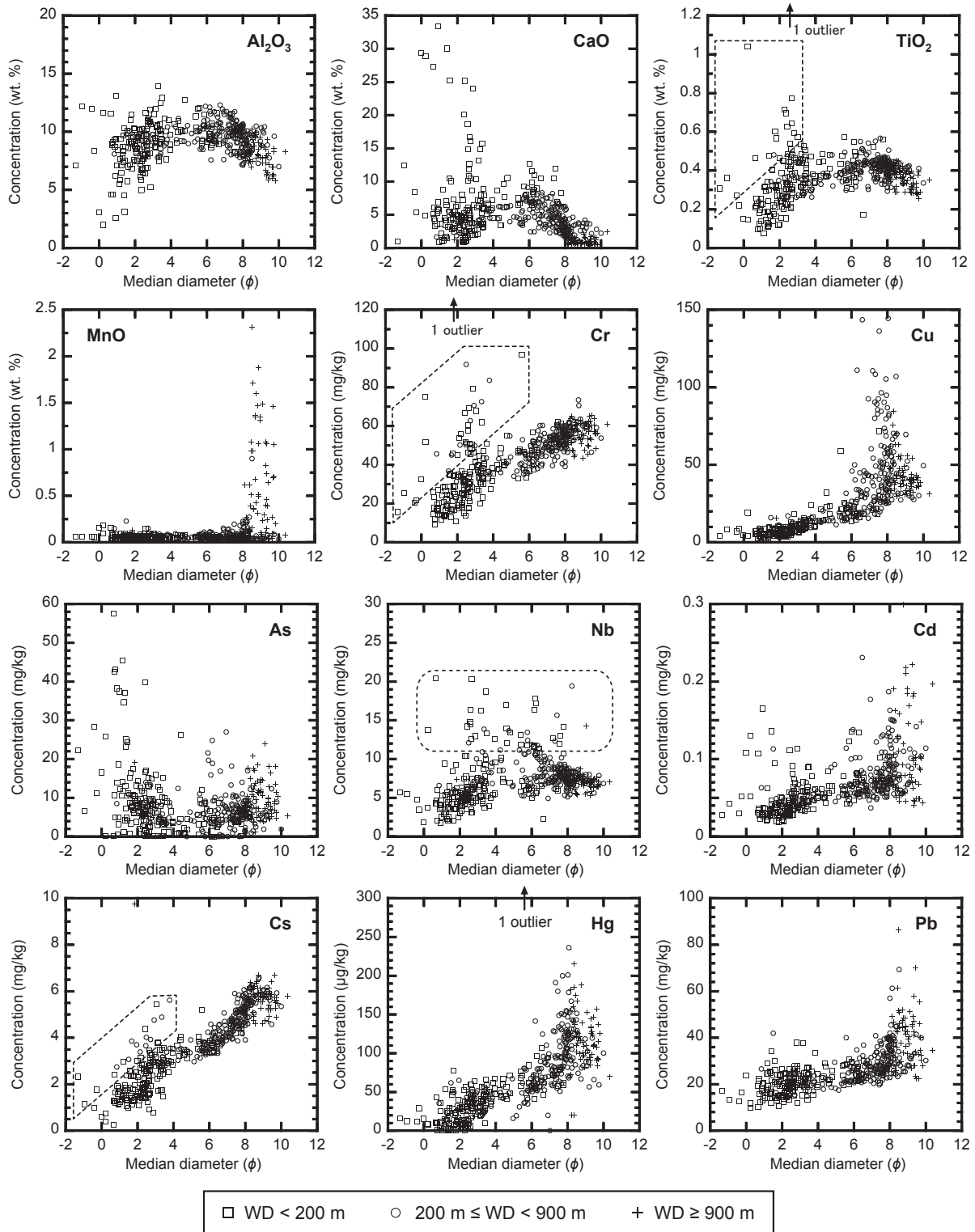
Fig. 3 The relationship between median diameter (Md (ϕ)) and elemental concentrations. The area enclosed by dotted lines indicates the samples that deviate from the positive correlation between Md(ϕ) and elemental concentration. Samples are classified into 3 groups according to water depth (WD): WD < 200 m (shelf), 200 m $\leq$ WD < 900 m (marginal terrace, slope, and sea topographic heights such as Oki ridge), and WD $\geq$ 900 m (trough).

Table 3 Median elemental concentrations of marine sediments and stream sediment data.

Element	Unit	Coarse sand (N=62)	Fine sand (N=112)	Silt (N=171)	Clay (N=115)	Land_sea side (N=130)
Li	mg/kg	24.2	32.2	48.6	57.2	29.8
Be	mg/kg	1.16	1.28	1.44	1.44	1.57
Na_2O	wt. %	2.35	2.41	2.95	4.31	2.27
MgO	wt. %	1.69	2.10	2.52	3.05	2.31
Al_2O_3	wt. %	8.66	9.08	10.0	8.47	10.9
P_2O_5	wt. %	0.093	0.099	0.144	0.150	0.127
K_2O	wt. %	1.98	2.10	1.93	1.93	1.99
CaO	wt. %	4.54	4.61	5.32	1.35	1.92
Sc	mg/kg	5.05	7.07	9.18	8.50	11.3
TiO_2	wt. %	0.238	0.347	0.422	0.391	0.699
V	mg/kg	38.8	41.0	57.0	75.8	106
Cr	mg/kg	22.2	34.1	49.1	57.0	67.5
MnO	wt. %	0.057	0.051	0.049	0.120	0.132
$T-Fe_2O_3$	wt. %	3.22	3.47	3.68	3.76	5.61
Co	mg/kg	6.52	7.45	8.14	10.7	14.2
Ni	mg/kg	10.0	12.8	25.4	35.8	26.9
Cu	mg/kg	5.31	8.90	27.5	41.5	29.2
Zn	mg/kg	42.9	59.1	88.3	101	124
Ga	mg/kg	11.1	12.4	14.2	14.2	17.7
As	mg/kg	10.7	6.0	5.7	7.5	9.3
Rb	mg/kg	70.2	71.9	68.8	73.5	77.4
Sr	mg/kg	328	283	257	133	147
Y	mg/kg	7.97	10.6	12.1	10.3	15.5
Zr	mg/kg	31.2	42.9	56.3	49.9	54.2
Nb	mg/kg	4.47	6.08	8.03	7.20	7.98
Mo	mg/kg	0.54	0.59	0.83	1.54	1.12
Cd	mg/kg	0.034	0.045	0.067	0.083	0.18
Sn	mg/kg	0.95	1.38	2.15	2.38	2.65
Sb	mg/kg	0.47	0.46	0.66	1.16	0.83
Cs	mg/kg	1.57	2.64	4.21	5.69	4.02
Ba	mg/kg	337	351	312	375	406
La	mg/kg	13.7	17.2	17.8	15.4	19.4
Ce	mg/kg	28.6	36.6	36.9	28.4	36.2
Pr	mg/kg	3.01	3.88	4.05	3.52	4.48
Nd	mg/kg	11.5	14.7	15.7	13.7	17.4
Sm	mg/kg	2.14	2.84	3.07	2.72	3.45
Eu	mg/kg	0.53	0.68	0.69	0.58	0.80
Gd	mg/kg	1.89	2.49	2.71	2.41	3.16
Tb	mg/kg	0.31	0.39	0.44	0.40	0.53
Dy	mg/kg	1.48	1.88	2.18	1.91	2.64
Ho	mg/kg	0.27	0.35	0.41	0.37	0.50
Er	mg/kg	0.78	1.00	1.19	1.05	1.44
Tm	mg/kg	0.12	0.16	0.19	0.17	0.22
Yb	mg/kg	0.76	0.99	1.17	1.03	1.40
Lu	mg/kg	0.11	0.14	0.17	0.16	0.20
Hf	mg/kg	0.88	1.16	1.48	1.31	1.56
Ta	mg/kg	0.39	0.53	0.75	0.67	0.60
Hg	µg/kg	13	34	74	116	50
Tl	mg/kg	0.41	0.49	0.50	0.51	0.54
Pb	mg/kg	18.5	20.4	26.5	36.2	25.2
Bi	mg/kg	0.18	0.21	0.45	0.69	0.27
Th	mg/kg	3.70	5.62	6.89	5.84	6.30
U	mg/kg	0.97	1.18	1.58	1.48	1.45

shows a concave feature. Some samples do not fall on the trends mentioned above. For example, V, MnO, Co, Mo, Cd, Sn, Sb, Pb, and Bi are highly enriched in deep sea sediments (WD ≥ 900 m) having Φ > 8. Factors other than grain size effects elevate their concentrations, and they will be discussed in detail in subsequent sections.

3.4 Terrestrial spatial distribution patterns of elemental concentrations

Spatial distribution patterns of elemental concentrations in terrestrial regions are influenced primarily by surface lithologies and sporadically by the presence of mineral deposits. Na_2O, Be, Ga, Nb, Y, Ln, Tl, Th, and U are abundant in stream sediments flowing in areas covered by granitic rocks. Mafic volcanic rocks elevate the concentrations of MgO, Sc, V, Cr, $T-Fe_2O_3$, Co, Ni, and Sr in stream sediments. MgO, Cr, Co, and Ni in particular are extremely enriched in stream sediments derived from mafic rocks of accretionary complexes and ultramafic rocks associated with Yakuno ophiolite. Li, MnO, Rb, Sb, Cs, and Tl concentrations are enhanced in stream sediments derived from sedimentary rocks of accretionary complexes. Geochemically anomalous areas having high concentrations of Cu, Zn, As, Mo, Cd, Sn, Sb, Hg, Pb, and Bi tended to be spatially related to the presence of mineral deposits (see star symbols in Fig. 2).

4. Discussion

4.1 Sandy sediments on the shelf: Contribution of river input and relict sediments

Although the input of terrigenous materials to coastal sea is not conspicuous, the supply of terrigenous materials to marine environment through the Yura River is clearly recognized in Wakasa Bay. The Yura River flows through an area covered by ultramafic, metabasalt, and gabbroitic rocks associated with accretionary complexes and Yakuno ophiolite that are highly abundant in MgO, TiO_2, Sc, V, Cr, $T-Fe_2O_3$, Co, and Ni (see TiO_2, Cr, and $T-Fe_2O_3$ in Fig. 2).

Al_2O_3, CaO, Sr, and Ga are abundant in Miho Bay (see Al_2O_3 and CaO in Fig. 2). The Hino and Hii Rivers supplied a large amount of decomposed granite soil to Miho Bay through large-scale mining of iron sand during 1600–1920. Therefore, high concentrations of Al_2O_3, Ca, Sr, and Ga indicate the spatial distribution of plagioclase. However, these high concentrations are restricted to Miho Bay and off Daisen volcano. This indicates that sandy sediments from rivers are deposited quite near shore.

Enrichment of Be, MgO, Al_2O_3, K_2O, Sc, V, TiO_2, $T-Fe_2O_3$, Co, Zn, Ba and Ln in sandy sediments is found on the shelf between Gentatsu-Se and the mouth of the Kuzuryu River (see plus symbols in TiO_2 map of Fig. 2). These sandy samples plot

off of the trend between TiO_2 and median diameter (Φ) (Fig. 3). These elements except for Be, K_2O, and Ln are also enriched in the adjacent terrestrial area where the Kuzuryu River flows. Katayama *et al.* (2000) reported that sandy sediments on the shelf contain amphibole, pyroxene and magnetite that originate from andesitic volcanic rocks in the catchment area of Kuzuryu River. Consequently, continuous spatial distribution of high concentrations of MgO, Al_2O_3, Sc, V, TiO_2, $T-Fe_2O_3$, Co, and Zn across land and sea is explained by the input of terrestrial materials to coastal sea. However, the spatial distributions of high Be, K_2O, Sc, V, $T-Fe_2O_3$, and Ln concentrations extend beyond this region and continue from Gentatsu-Se to Wakasa Basin. In addition, the area corresponds to the distribution of sandy sediments that plot outside the trend between Cr and Cs concentrations and median diameter (Φ) (see Cr and Cs data in the area enclosed by dotted lines in Fig. 3). Those elements are not abundant in the catchment area of Kuzuryu River (Fig. 2). Those results support the suggestion that the sandy sediments located off Gentatsu-Se are denudated from old sediments (Ikehara *et al.*, 1990a; Katayama *et al.*, 2000).

4.2 Input of Oki Island volcanic material to the southeast of the Oki Islands and near the Oki Ridge and Wakasa Sea Knoll Chain

Li, Sc, Cu, Ni, Zn, Ga, Cs, Sn, Cd, Pb, Hg, Bi, Tl, and U are enriched in the small basins and marginal terrace around the Oki Islands, which are covered by silty and clayey sediments (6 < Φ < 9). Because those elements are not abundant in the stream sediments of Oki Islands, their enrichments are explained simply by grain size effects.

In contrast, samples having high Be, TiO_2, Zr, Nb, Y, Ln, Th, and U concentrations are found around the Oki islands, Oki Ridge, and Wakasa Sea Knoll Chain. Samples enriched in Nb, Y, Ln, Ta, Th, and U have a variety of grain sizes but their distribution is restricted to the western part of the shallow waters (see the samples enclosed by dotted line in Nb of Fig. 3). Yamasaki (1998) reported that the crust of the Oki Islands is considered to be a fragment of continental crust. The Oki island area including Oki Spur and Oki Strait were formed by a complex evolutionary process and covered heavily by lavas and pyroclastic rocks during the late Miocene and Pleistocene. Alkali-rhyolite is dominant in the eastern Oki Islands and alkali-basalt is dominant in the western Oki Islands. They are enriched in incompatible elements such as Zr, Nb, and rare earth elements compared with non-alkaline volcanic rocks distributed on the mainland (Kaneko, 1991; Kobayashi *et al.*, 2002). River sediments from the Oki Islands are also enriched in these elements. However, the Oki islands are small islands so the supply of the volcanic materials through rivers would be subtle. Marine geological maps indicate that Quaternary alkali-basaltic rock and

Pliocene tuffaceous sandstone and volcanic rocks are distributed widely and exposed in the shallow waters (WD < 100 m) around the Oki Islands and Oki Spur (Tamaki *et al*., 1982). Erosion and denudation processes acting on the seabed by tidal waves would produce sandy and silty sediments that could then be subsequently dispersed by a branch current of the Tsushima Current.

Sandy sediments around the Oki Ridge and Wakasa Sea Knoll Chain are enriched in Be, K_2O, Sc, Cr, Rb, Y, Zr, Nb, Ba, Ln, Hf, Ta, and Th. Ikehara *et al*. (1990a) suggested that sandy sediments around Oki Ridge contain a large amount of volcanic glass, volcanic fragments, and pumice. Yamamoto *et al*. (1990) reported that semi-consolidated silt, andesitic welded tuff associated with moonstone, alkali-rhyolites, and pumices were dredged from the top and southern slope of Oki Ridge. These volcanic rocks are also found in the Oki Islands. As we explained above, that region has a low deposition rate or is in an erosional regime. Therefore, the enrichment of the above elements is explained by sands denudated from alkaline olivine basalt.

The elements Sc, Ti, Nb, Y, Ln, Ta, and Th are used for the discrimination of sediments because they are relatively immobile in nature. Yang *et al*. (2003) used the concentration ratios of Cr/Th, Ti/Nb, and La/Yb as geochemical parameters for a provenance study of Yellow Sea sediments. In the study area, Sc and TiO_2 are roughly abundant in the eastern region except for samples located near the Oki Islands, whereas Nb, Y, Ln, Ta, and Th are abundant in sediments around the Oki Islands. Therefore, the ratio of the former and latter elements is useful to elucidate the dispersion process of alkaline volcanic materials. Figure 4 shows how Ti/Nb and Sc/La ratios classified by grain size (sand, silt, and clay) change from west to east. For comparison, these ratios in stream sediments collected from rivers flowing into the Sea of Japan and from Oki Islands ($N = 138$) are also shown in Fig. 4.

The Ti/Nb and Sc/La ratios in stream sediments vary widely. The former ratio gradually increases toward the east but the latter ratio is almost constant. Stream sediments collected from the Oki Island have the lowest ratios among stream sediments in the study area: Ti/Nb = 85−260 and Sc/La = 0.10−0.48. Sandy sediments on the shelf have a similar trend to stream sediments. Their Ti/Nb and Sc/La ratios are consistent with the lowest values of stream sediments. This fact suggests that mineralogical composition in sediments is largely fractionated between river and coastal sea. It is apparent that these sandy shelf sediments seem to be affected by river sediments rather than alkaline volcanic rocks, except for samples collected from the Oki Islands.

In contrast, both Ti/Nb and Sc/La ratios in silty sediments are low at 133° E, gradually increase toward the east, and finally level out to constant values between 135.4° E and 136.8° E (Fig. 4). Ikehara (1991) suggested that fine particles selectively deposit around current rips and between surface water and deep water. In this study area, muddy sediments deposit on the marginal terrace (WD = 200−500 m), near a water mass boundary between the Tsushima Current (surface water) and JSPW (deep sea). Therefore, the spatial distribution of silty sediments on the marginal terrace is strongly affected by the oceanic current. The systematic changes of Ti/Nb and Sc/La ratios from west to east (between 133° E and 135.4° E) indicate that silty grains originating from alkaline volcanic rocks are conveyed by the Tsushima Current or related bottom sea flows along the marginal terrace for distances as far as 200 km.

Finally, clay sediments have constant ratios of Ti/Nb and Sc/La along the east-west direction different from the cases of sandy and silty sediments. The reason is that clay minerals are weathering products of other minerals, resulting in the loss of their original geochemical features.

4.3 Influence of early diagenetic processes and input of organic materials in silt and clay

The elements MnO, V, Ni, Co, Mo, Sb, Pb, and Bi are extremely enriched in deep basins with water depths below 900 m and which are covered by clay ($Md(\Phi) > 8$). ORP is positive in the Oki Trough and a brown clay layer is found at the top of surface sediments (0 − 4 cm) of Oki Trough (Fig. 2) (Ikehara *et al*., 1990a; Katayama *et al*., 1993). The brown clay layer is considered to be the oxidizing layer and the result of Mn oxide precipitation. The enrichments of V, Ni, Co, Mo, Sb, Pb, and Bi may therefore be caused by early diagenetic processes (e.g., Klinkhammer, 1980; Shaw *et al*., 1990). This process involves metals that are dissolved at greater depths in sediments under reducing conditions, then diffuse upward, and finally precipitate with Fe-Mn hydroxides, especially Mn dioxide, or on the sediment surface under oxic conditions (Aplin and Cronan, 1985; Shaw *et al*., 1990; Morford *et al*., 2005). Actually, Yin *et al*. (1989) confirmed that MnO and Co in brownish muds of the Oki trough and Tsushima Basin exist in the form of Fe-Mn oxides or hydroxides through extraction experiment.

Although V, Co, Ni, Mo, and Sb concentrations in clay sediments of the study area correlate positively to the concentration of MnO, their relationship is fairly scattered (Fig. 5). Provided that enrichment of MnO, V, Ni, Co, Mo, Sb, Pb, and Bi was caused by early diagenetic processes under a static depositional environment, their concentrations would have a definite correlation with MnO concentration. Ikehara *et al*. (1990b) suggested that the southwestern part of Oki Trough is covered by mass-transport deposits derived from slope failure at the edge of the marginal terrace and the northeast part is covered
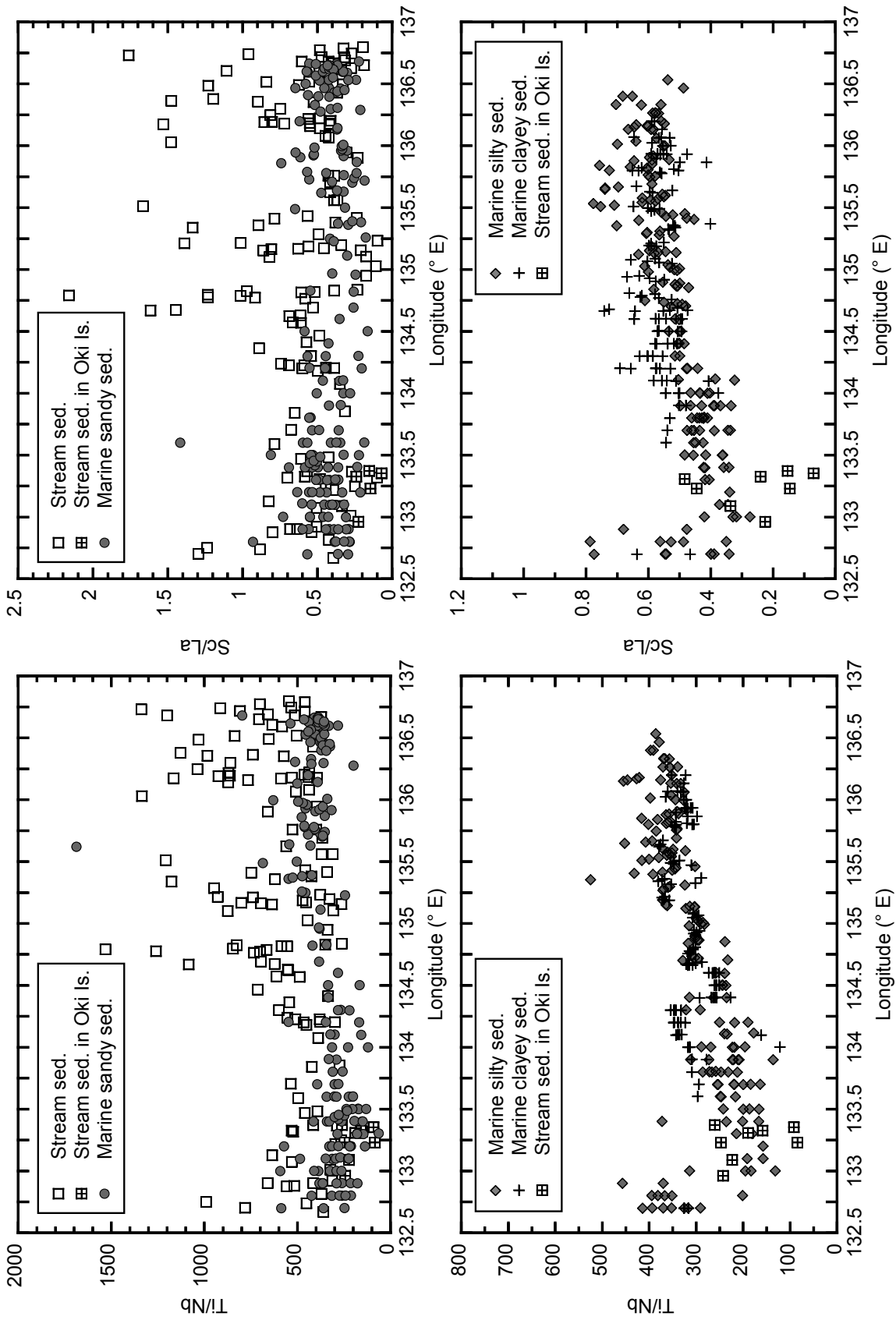
Fig. 4 The longitudinal dependence of Ti/Nb and Sc/La ratios in marine sediments (sandy, silty, and clayey sediments) and stream sediments.
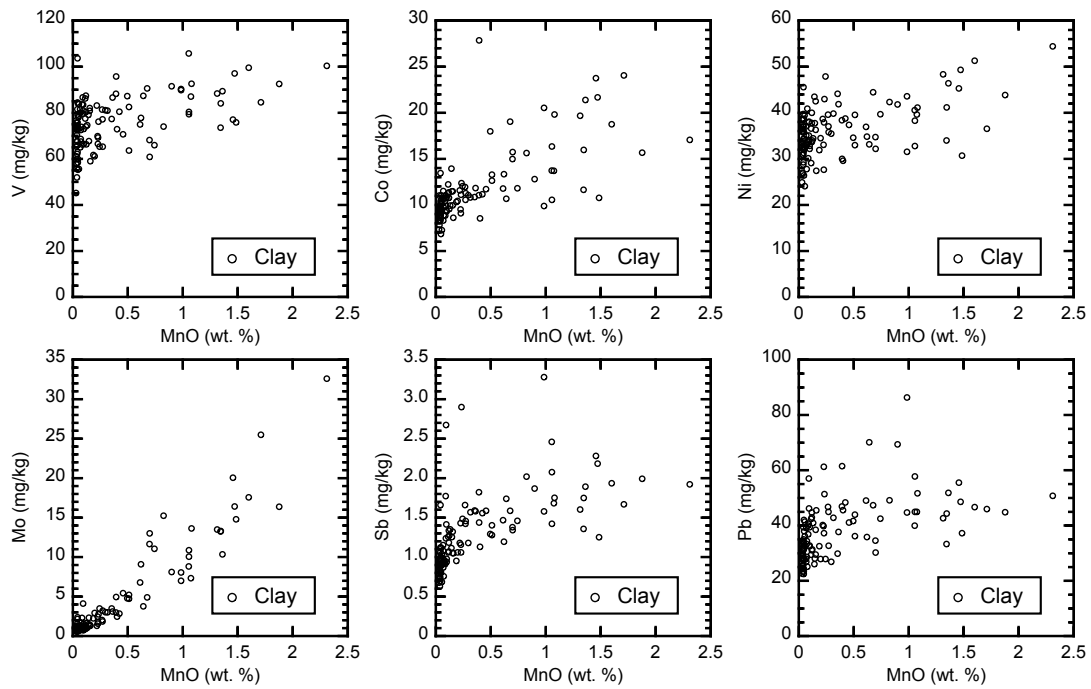
Fig. 5 Scatter diagrams of elemental concentrations in the marine sediments classified as clay ($\phi > 8$).
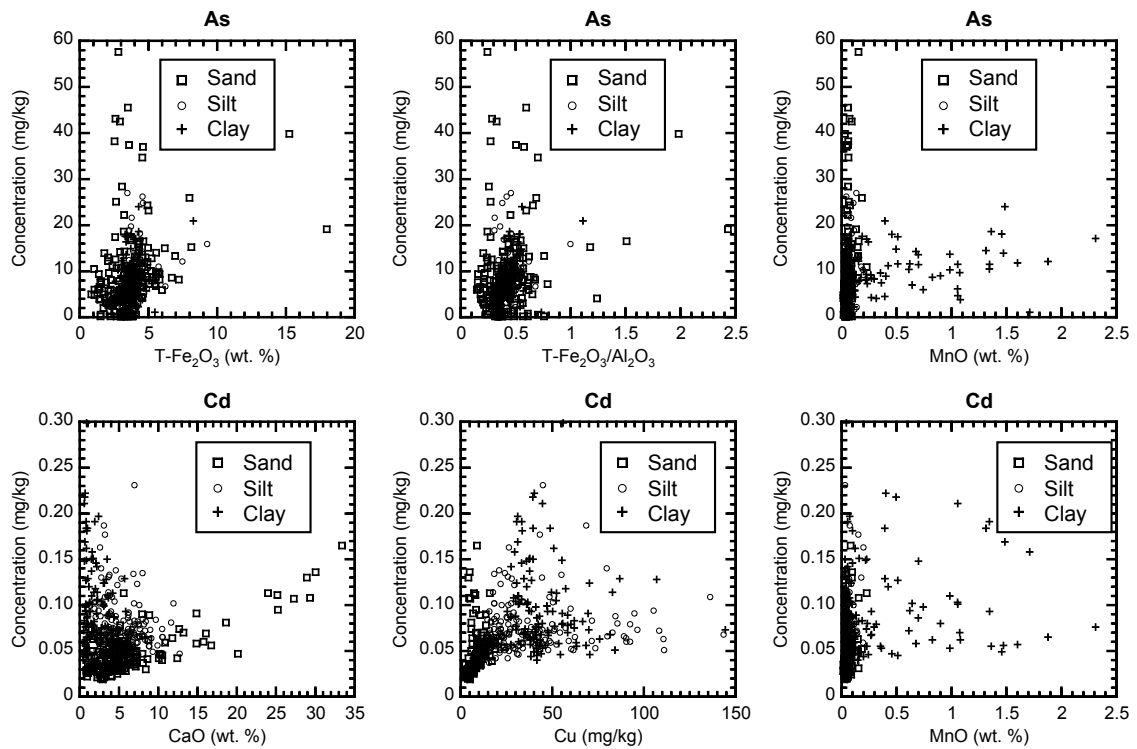

Fig. 6 Scatter diagrams of elemental concentrations in the marine sediments (sand, silt, and clay).

by hemi-pelagic deposition based on seismic records. In other words, sedimentation in Oki Trough and Wakasa Basin has been frequently interrupted by turbidity flow. In that case, early diagenetic process is re-started after the event (Wilson *et al.*, 1985). Such an episodic event may disturb the correlation among MnO, V, Ni, Co, Mo, Sb, Pb, and Bi concentrations in clay sediments.

Silt and clay samples distributed on the marginal terrace and the slope (WD = 200 – 900 m) are also enriched in Ni, Cd, Mo, Sn, Sb, Pb, and Bi, especially in Cu, Zn and Hg (see Cu and Hg in Fig. 3). Their enrichment cannot be explained simply by early diagenetic processes.

The marginal terrace and the slope have negative ORP (under reductive condition) different from deep sea basin (Fig. 2): It has been known that Cu and Hg are transported with detrital biogenic materials from shallow water to sediments (Bothner *et al.*, 1980; Klinkhammer, 1980; Shaw *et al.*, 1990; Mason *et al.*, 1994). They are released from surface sediments to seawater during decomposition of organic matter or are associated with residual organic matter. Namely, the organic remains are an important source of elements in deep seas.

The deposition rate on the marginal terrace is very high (about 10 – 25 cm/1000y) (Ikehara, 1991). In that place, organic materials associated with silt and clay are also deposited in abundance on the marginal terrace and the slope. They would increase the oxygen consume during the decomposition and cause reducible condition (see ORP data in Fig. 2a). As a result, the organic remaining on the marginal terrace and the slope elevates the concentrations of Cu, Zn and Hg.

Furthermore, the Cu, Zn and Hg concentrations on the marginal terrace and the slope gradually increase toward the east (see Cu and Hg in Fig. 3). Actually, the mean concentration ratios of Cu, Zn and Hg in the east part (between 132.5° E and 134.5° E) to those in the west part (between 134.5° E and 135.4° E) are calculated to be 1.9, 1.3, and 1.6, respectively. Correspondingly, the eastern marginal terrace has ORP values of approximately −50 to −180 eV, with absolute values larger than those found on the western marginal terrace (Fig. 2). Katayama *et al.* (1993) reported that the deposition rate on the eastern marginal terrace is larger than that on the western side based on the seismic records. From those reasons, we assumed that there were many supplies of organic materials in the eastern side.

4.4 Controlling factors of spatial distribution patterns of As and Cd

The spatial distribution patterns of As and Cd somewhat differ from the above mentioned elements. As is abundant in both shelf and basin, Cd is sporadically enriched in the marginal terrace, slope, and basins. The spatial distribution patterns of

As concentration and ORP show that As is high in shelf sediments where its oxic conditions are dominant. Brown or brownish-black sands that contain quartz coated by Fe hydroxides are distributed widely on shelf, especially on the eastern margin of Oki Strait and the shelf off the Noto Peninsula (see cross symbols plotted in As map of Fig. 2) (Ikehara *et al.*, 1990a; Katayama *et al.*, 2000). Fe hydroxide-coated quartz grains would absorb As efficiently (Belzile and Tessier, 1990; Sullivan and Aller, 1996; Chaillou *et al.*, 2008). However, As concentration correlates with neither T-Fe$_2$O$_3$ concentration nor the T-Fe$_2$O$_3$/Al$_2$O$_3$ (or T-Fe$_2$O$_3$/TiO$_2$) ratio, with some exceptions (Fig. 6). In addition, no enrichment of As is found in the adjacent terrestrial area: Sendai, Kuzuryu, and Tetori river systems. Therefore, Fe hydroxide coats minerals thinly and would have absorbed As dissolved in water over a long period. Furthermore, clayey sediments in the Oki Trough are abundant in As (Fig 3). Because their As concentrations roughly correlate to MnO ones (Fig. 6), enrichment of As in the Oki Trough would be caused by early diagenetic process.

Sediments having high Cd concentration are found ubiquitously: on the shelf, marginal terrace and in basins. The relatively high Cd concentration of coarse sediments on the shelf is explained by calcareous materials because Cd^{2+} has a similar ionic radius to Ca^{2+}. Figure 6 shows that CaO concentration in sediments associated with calcareous materials positively correlates with Cd concentration. By contrast, Cd concentrations of silty and clayey sediments do not correlate with Cu and MnO concentrations (Fig. 6), whose concentrations indicate the influences of metal binding with organic matters and early diagenetic process, respectively. The geochemistry of Cd is opposite to Mn, V, Ni, Co, Mo, Sb, Pb, and Bi during early diagenetic processes and authigenically accumulates in sediments (for example by precipitation as CdS) (Rosenthal *et al.*, 1995; Morford *et al.*, 2005; Chaillou *et al.*, 2008). For these reasons, Cd does not bind to organic materials and Mn oxides, but authigenically accumulates in silty and clayey sediments.

5. Conclusions

A comprehensive examination of the spatial distribution of 53 elements of 460 marine sediments in the western side of the Sea of Japan and 254 stream sediments collected from the adjacent terrestrial area has been conducted. The spatial distribution of elemental concentrations in marine sediments is influenced by many factors: (1) grain size effects (including dilution effects), (2) particle transport from the land to coastal seas, (3) biogenic remains, (4) conveyance of coastal sediments by waves and coastal currents, (5) early diagenetic processes, (6) deposition at water mass boundaries, (7) denudation or resedimentation of

basement rocks, and (8) precipitation of Fe−Mn oxides. These controlling factors closely relate to marine geography, water depth, and depositional environment.

The influence of particle transport from land to seas through river systems is observed only in restricted area. This is because strong tidal waves and coastal currents sweep away fine grains on the shelf that are supplied from rivers. As a result, old sandy sediments are distributed widely on the shelf. Most elements have low concentrations in sandy sediments because of dilution effects by quartz and calcareous materials. Quartz in relict sediments is often coated by Fe hydroxides and effectively absorbs As. Calcareous materials such as shell fragments and foraminifera cause not only enrichment of CaO, and Sr but also enrichment of Cd. Sea topographic highs (Oki Ridge, Wakasa Sea Knoll Chain, and Gentatsu-Se) are covered by sandy sediments that are produced by denudation or resedimentation of basement rocks. Their elemental abundances are different from the sediments in the surrounding areas.

Silty sediments are deposited on the marginal terrace where a water mass boundary is located. The spatial distribution patterns of Y, Nb Ln, Ta, and Th clearly suggest that silty sediments denudated from alkaline volcanic rocks around the Oki Islands are conveyed toward the east and deposited on the marginal terrace. In the eastern marginal terrace, Cu, Zn, and Hg are enhanced in silty sediments associated with biogenic remains. In contrast, the deep sea is covered by a low-temperature and oxygen-rich water mass (Japan Sea Proper Water), so that clay sediments distributed there rarely contain calcareous materials and organic remains. A brown clay layer associated with Mn oxide precipitation is found in deep sea basins and is highly enriched in V, Co, Ni, Mo, Sb, Pb, and Bi because of early diagenetic processes.

Acknowledgments

References

Akimoto, T., Kawagoe, S. and Kazama, S. (2009) Estimation of sediment yield in japan by using climate projection model. *Proceedings of Hydraulic Engineering*, **53**, 655-660 (In Japanese with English abstract).

Aplin, A. C. and Cronan, D. S. (1985) Ferromanganese oxide deposits from the Central Pacific Ocean .I. Encrustations from the Line Islands Archipelago. *Geochim. Cosmochim. Acta*, **49**, 427-436.

Belzile, N. and Tessier, A. (1990) Interactions between arsenic and iron oxyhydroxides in lacustrine sediments. *Geochim. Cosmochim. Acta*, **54**, 103-109.

Bothner, M. H., Jahnke, R. A., Peterson, M. L. and Carpenter, R. (1980) Rate of mercury loss from contaminated estuarine sediments. *Geochim. Cosmochim. Acta*, **44**, 273-285.

Chaillou, G., Schäfer, J., Blanc, G. and Anschutz, P. (2008) Mobility of Mo, U, As, and Sb within modern turbidites. *Mar. Geol.*, **254**, 171-179.

Darnley, A. G., Björklund, A., Bølviken, B., Gustavsson, N., Koval, P. V., Plant, J. A., Steenfelt, A., Tauchid, M., Xie, X., Garrett, R. G. and Hall, G. E. M. (1995) *A global geochemical database for environmental and resource management: recommendations for international geochemical mapping*. UNESCO Publishing, Paris, 122 pp.

De Vos, W., Tarvainen, T., Salminen, R., Reeder, S., De Vivo, B., Demetriades, A., Pirc, S., Batista, M. J., Marsina, K., Ottesen, R.-T., O'Connor, P. J., Bidovec, M., Lima, A., Siewers, U., Smith, B., Taylor, H., Shaw, R., Salpeteur, I., Gregorauskiene, V., Halamic, J., Slaninka, I., Lax, K., Gravesen, P., Birke, M., Breward, N., Ander, E. L., Jordan, G., Duris, M., Klein, P., Locutura, J., Bel-lan, A., Pasieczna, A., Lis, J., Mazreku, A., Gilucis, A., Heitzmann, P., Klaver, G. and Petersell, V. (2006) *Geochemical atlas of Europe. Part 2 - Interpretation of Geochemical Maps, Additional Tables, Figures, Maps, and Related Publications*. Geological Survey of Finland, Espoo, Finland, 692 pp.

Gamo, T., Nozaki, Y., Sakai, H., Nakai, T. and Tsubota, H. (1986) Spatial and temporal variations of water characteristics in the Japan Sea bottom layer. *J. Mar. Res.*, **44**, 781-793.

Geological Survey of Japan (1992) *Geological Map of Japan, 1:1,000,000 (3rd, ed.)*. Geol. Surv. Japan.

Howarth, R. J. and Thornton, I. (1983) Regional Geochemical Mapping and its Application to Environmental Studies. *In* Thornton, I., ed., *Applied Environmental Geochemistry*, Academic Press, London, 41-73.

Ikehara, K. (1991) Modern sedimentation off san in district in the southern Japan Sea. Oceanography of Asian Marginal Seas, 143-161.

Ikehara, K. (2010) *Sedimentological Map of Oki Strait*. 1:200,000 Marine Geology Map Series 69 (CD-ROM version), Geol. Surv. Japan, AIST.

Ikehara, K., Katayama, H. and Satoh, M. (1990a) *Sedimentological Map offshore of Tottori*. 1:200,000 Marine Geology Map Series 36, Geol. Surv. Japan, AIST.

Ikehara, K., Satoh, M. and Yamamoto, H. (1990b) Sedimentation in the Oki Trough, southern Japan Sea, as revealed by high

resolution seismic records (3.5 kHz echograms). *Jour. Geol. Soc. Japan*, **96**, 37-49.

Imai, N., Terashima, S., Ohta, A., Mikoshiba, M., Okai, T., Tachibana, Y., Togashi, S., Matsuhisa, Y., Kanai, Y. and Kamioka, H. (2010) *Elemental distribution in Japan -Geochemical map of Japan-*. (Imai, N., ed.). Geol. Surv. Japan, AIST, Tsukuba.

Iwabuchi, Y. (1968) Submarine geology of the southeastern part of the Japan Sea. *Contributions from the Institute of Geology and Paleontology Tohoku University*, **66**, 1-76 (In Japanese with English abstract).

Iwabuchi, Y. and Kato, S. (1988) Some features of the continental shelf around the Japanese Islands on compilation of *the Quaternary Map. The Quaternary Research (Daiyonki-Kenkyu)*, **26**, 217-225 (In Japanese with English abstract).

Kaneko, N. (1991) Petrology of Oki-Dozen volcano. Part 1. Petrography and, major and trace element compositions. *J. Min. Petr. Econ. Geol.*, **86**, 140-159 (In Japanese with English abstract).

Katayama, H. and Ikehara, K. (2001) *Sedimentological Map west of Noto Peninsula*. 1:200,000 Marine Geology Map Series 57, Geol. Surv. Japan, AIST.

Katayama, H., Mikio, S. and Ikehara, K. (1993) *Sedimentological Map offshore of Kyo-ga Misaki*. 1:200,000 Marine Geology Map Series 38, Geol. Surv. Japan, AIST.

Katayama, H., Mikio, S. and Ikehara, K. (2000) *Sedimentological Map of Gentatsu-Se*. 1:200,000 Marine Geology Map Series 53, Geol. Surv. Japan, AIST.

Klinkhammer, G. P. (1980) Early diagenesis in sediments from the eastern equatorial Pacific. II. Pore water metal results. *Earth Planet. Sci. Lett.*, **49**, 81-101.

Kobayashi, S., Sawada, Y. and Yoshida, T. (2002) Magma plumbing systems of the Latest Miocene Oki Alkaline Volcanic Group, Oki-Dogo Island, SW Japan, based on geology and petrology. *Japanese Magazine of Mineralogical and Petrological Sciences*, **31**, 137-161 (In Japanese with English abstract).

Kondo, H. (2006) Lipid Compounds and Distribution in Sediments from Tango-kai Bay of western part of Wakasa Bay. *Bulletin of Faculty of Education, Nagasaki University. Natural science*, **74**, 15-25.

Mason, R. P., Fitzgerald, W. F. and Morel, F. M. M. (1994) The biogeochemical cycling of elemental mercury: Anthropogenic influences. *Geochim. Cosmochim. Acta*, **58**, 3191-3198.

Morford, J. L., Emerson, S. R., Breckel, E. J. and Kim, S. H. (2005) Diagenesis of oxyanions (V, U, Re, and Mo) in pore waters and sediments from a continental margin. *Geochim. Cosmochim. Acta*, **69**, 5021-5032.

Naganuma, K. (1977) The Oceanographic fluctuations in the Japan Sea. *Marine sciences monthly*, **9**, 137-141 (In Japanese with English abstract).

Ohta, A. and Imai, N. (2011) Comprehensive Survey of Multi-Elements in Coastal Sea and Stream Sediments in the Island Arc Region of Japan: Mass Transfer from Terrestrial to Marine Environments. *In* El-Amin, M., ed., *Advanced Topics in Mass Transfer*, InTech, Available from: http://www.intechopen.com/books/advanced-topics-in-mass-transfer/comprehensive-survey-ofmulti-elements-in-coastal-sea-and-stream-sediments-in-the-island-arc-region, Croatia, 373-398.

Ohta, A., Imai, N., Terashima, S., Tachibana, Y., Ikehara, K. and Nakajima, T. (2004) Geochemical mapping in Hokuriku, Japan: influence of surface geology, mineral occurrences and mass movement from terrestrial to marine environments. *Appl. Geochem.*, **19**, 1453-1469.

Ohta, A., Imai, N., Terashima, S., Tachibana, Y., Ikehara, K., Okai, T., Ujiie-Mikoshiba, M. and Kubota, R. (2007) Elemental distribution of coastal sea and stream sediments in the island-arc region of Japan and mass transfer processes from terrestrial to marine environments. *Appl. Geochem.*, **22**, 2872-2891.

Ohta, A., Imai, N., Terashima, S., Tachibana, Y., Ikehara, K., Katayama, H. and Noda, A. (2010) Factors controlling regional spatial distribution of 53 elements in coastal sea sediments in northern Japan: Comparison of geochemical data derived from stream and marine sediments. Appl. Geochem., **25**, 357-376.

Ohta, A., Imai, N., Terashima, S., Tachibana, Y. and Ikehara, K. (2013) Regional spatial distribution of multiple elements in the surface sediments of the eastern Tsushima Strait (southwestern Sea of Japan). Appl. Geochem., **37**, 43-56.

Reimann, C. (2005) Geochemical mapping: technique or art? Geochem.: Explor. *Environ. Anal.*, **5**, 359-370.

Rosenthal, Y., Lam, P., Boyle, E. A. and Thomson, J. (1995) Authigenic cadmium enrichments in suboxic sediments: Precipitation and postdepositional mobility. *Earth Planet. Sci. Lett.*, **132**, 99-111.

Salminen, R., Batista, M. J., Bidovec, M., Demetriades, A., B., D. V., De Vos, W., Duris, M., Gilucis, A., Gregorauskiene, V., Halamic, J., Heitzmann, P., Lima, A., Jordan, G., Klaver, G., Klein, P., Lis, J., Locutura, J., Marsina, K., Mazreku, A., O'Connor, P. J., Olsson, S. Å., Ottesen, R.-T., Petersell, V., Plant, J. A., Reeder, S., Salpeteur, I., Sandström, H., Siewers, U., Steenfelt, A. and Tarvainen, T. (2005) *Geochemical atlas of Europe. Part 1 - Background Information, Methodology and Maps*. Geological Survey of Finland, Espoo, Finland, 526 pp.

Senjyu, T., Shin, H. R., Yoon, J. H., Nagano, Z., An, H. S., Byun, S. K. and Lee, C. K. (2005) Deep flow field in the Japan/East Sea as deduced from direct current measurements. *Deep-Sea Res. Part II-Top. Stud. Oceanogr.*, **52**, 1726-1741.

Shaw, T. J., Gieskes, J. M. and Jahnke, R. A. (1990) Early diagenesis in differing depositional environments: The response of transition metals in pore water. *Geochim. Cosmochim. Acta*, **54**, 1233-1246.

Sudo, H. (1986) A note on The Japan Sea Proper Water. *Prog. Oceanogr.*, **17**, 313-336.

Sullivan, K. A. and Aller, R. C. (1996) Diagenetic cycling of arsenic in Amazon shelf sediments. *Geochim. Cosmochim. Acta*, **60**, 1465-1477.

Tamaki, K., Yuasa, M. and Murakami, F. (1982) Geological Map of Oki Strait. 1:200,000 Marine Geology Map Series 20.

Watson, D. F. and Philip, G. M. (1985) A refinement of inverse distance weighted interpolation. *Geo-Processing*, **2**, 315-327.

Weaver, T. A., Broxton, D. E., Bolivar, S. L. and Freeman, S. H. (1983) *The Geochemical Atlas of Alaska: Compiled by the Geochemistry Group, Earth Sciences Division, Los Alamos National Laboratory*. GJBX-32(83), Los Alamos, 57 pp.

Webb, J. S., Thornton, I., Thompson, M., Howarth, R. J. and Lowenstein, P. L. (1978) *The Wolfson Geochemical Atlas of England and Wales*. Clarendon Press, Oxford, 69 pp.

Wilson, T. R. S., Thomson, J., Colley, S., Hydes, D. J., Higgs, N. C. and Sorensen, J. (1985) Early organic diagenesis: The significance of progressive subsurface oxidation fronts in pelagic sediments. *Geochim. Cosmochim. Acta*, **49**, 811-822.

Yamamoto, H. (1991) A submarine sediment slide on the continental slope off Fukui Prefecture, Southern Japan Sea. *Bull. Geol. Surv. Japan*, **42**, 221-232 (In Japanese with English abstract).

Yamamoto, H. (1993) Submarine geology and post-opening tectonic movements in the southern region of the Sea of Japan. *Mar. Geol.*, **112**, 133-150.

Yamamoto, H., Joshima, M. and Kisimoto, K. (1990) *Geological Map of Offshore of Tottori*. 1:200,000 Marine Geology Map Series 35, Geol. Surv. Japan.

Yamasaki, H. (1998) Late Cenozoic tectono-sedimentary history in the Oki-Dogo Island, and its implication for the origin of topographic and structural relief in the Southwestern Japan Sea. *Bulletin of the Faculty of School Education, Hiroshima University. Part II*, **20**, 85-153 (In Japanese with English abstract).

Yang, S. Y., Jung, H. S., Lim, D. I. and Li, C. X. (2003) A review on the provenance discrimination of sediments in the Yellow Sea. *Earth-Sci. Rev.*, **63**, 93-120.

Yin, J., Okada, H. and Labeyrie, L. (1987) Clay mineralogy of slope sediments around the Japanese Islands. *Geosci. Repts. Shizuoka Univ.*, **13**, 41-65.

Yin, J. H., Kajiwara, Y. and Fujii, T. (1989) Distribution of transition-elements in surface sediments of the southwestern margin of Japan Sea. *Geochem. J.*, **23**, 161-180.

隠岐トラフ周辺海域及び近接陸域における表層堆積物の元素分布：
特に日本海固有水のシルト質および粘土質堆積物への強い影響

太田充恒・今井 登・寺島 滋・立花好子・池原 研・片山 肇

要　旨

　全国陸域地球化学図に続く海域地球化学図プロジェクトにおいて，日本海西部海域から460個の海洋堆積物が採取され，53元素の分析がなされている．これら海洋堆積物の粒径や化学組成は堆積環境ごと(陸棚，縁辺台地，斜面，海盆など)で大きく異なる．まず陸棚上砂質堆積物の特徴として，主たる起源物質と考えられる(隣接地域の)河川堆積物の化学的特徴を反映していないことが挙げられる．陸棚の堆積物の多くは，鉄水酸化物で覆われた石英を多く含みかつヒ素に著しく富む特徴を有する．この特徴から，陸棚試料の多くは海退期－海進期に形成された残留堆積物が主で，現世の河川堆積物の寄与が小さいと考えられる．縁辺台地の堆積物の特徴として，現世のシルト質堆積物で広く覆われていることが挙げられる．これは，対馬海流(表層水)と日本海固有水(深層水)の境界が縁辺台地上(水深200–500 m)に位置しており，細粒なシルト質堆積物がこの水塊境界部で選択的に沈殿しているためである．西部縁辺台地のシルト質堆積物は，ニオブ，希土類元素，タンタル，トリウムなどに富んでおり，恐らく第四紀のアルカリ火山岩の削剥物の供給があったことを意味している．これらの堆積物は海流の影響を受けて200 kmほど東方へ運ばれていることが明らかとなった．一方，縁辺台地東方部においては，シルト質堆積物は銅，亜鉛，水銀などに富む特徴を有し，恐らく堆積物中の残留生物源物質の影響(有機物と結合して存在している)を見ていると考えられる．粘土質堆積物は隠岐トラフや海盆域に広く分布し，日本海固有水の影響を受けて，半遠洋性の非常に酸化的な環境下にある．堆積物表層部(0–4 cm)には，初期続成作用に伴う薄いマンガン酸化物層が認められ，バナジウム，コバルト，ニッケル，モリブデン，アンチモン，鉛を多く含む．このように，本調査海域の海洋堆積物の化学組成は，堆積環境に強く影響を受けていることが明らかとなった．